Journal of Orthopaedic Translation (2016) 6, 34—41

Available online at www.sciencedirect.com

ScienceDirect

journal homepage: http://ees.elsevier.com/jot

ORIGINAL ARTICLE

Comparison of three approaches for defining nucleus pulposus and annulus fibrosus on sagittal magnetic resonance images of the lumbar spine

Greta S.P. Mok [a], Duo Zhang [a], Shu-Zhong Chen [b], Jing Yuan [c], James F. Griffith [b], Yi Xiang J. Wang [b,*]

[a] *Biomedical Imaging Laboratory, Department of Electrical and Computer Engineering, University of Macau, Macau Special Administrative Region*
[b] *Department of Imaging and Interventional Radiology, Prince of Wales Hospital, The Chinese University of Hong Kong, Shatin, Hong Kong Special Administrative Region*
[c] *Medical Physics and Research Department, Hong Kong Sanatorium and Hospital, Happy Valley, Hong Kong Special Administrative Region*

Received 19 July 2015; received in revised form 8 February 2016; accepted 22 February 2016
Available online 22 April 2016

KEYWORDS
annulus fibrosus;
degeneration;
disc;
magnetic resonance imaging;
nucleus pulposus;
region of interest

Summary *Objective:* To compare three methods commonly used in the literature to define intervertebral disc nucleus pulposus (NP) and annulus fibrosus (AF) on magnetic resonance (MR) images.
Methods: Fifty-two patients (26 males and 26 females; age range, 23—76 years) were recruited for this study; they underwent standard T1/T2-weighted MR imaging, and T2 and T1rho mapping acquisitions. The corresponding midsagittal images were analysed and a total of 256 discs were evaluated, using three different region-of-interest (ROI) drawing methods: (1) radiologist-guided manual ROI (M-ROI); (2) five square ROIs where each measured 20% of the midline disc diameter (5-ROI); and (3) seven square ROIs placed horizontally from anterior to posterior (7-ROI) to define NP and AF. The agreement between the three ROI methods was assessed using intraclass correlation coefficient values and Bland—Altman plots.
Results: Inner AF and NP could not be differentiated on T1/T2-weighted MR imaging, T2 maps, or T1rho maps. The intraclass correlation coefficient values were all > 0.75 when comparing the 5-/7-ROI methods with the M-ROI methods for NP, and 0.167—0.488 for AF when comparing the 7-ROI method with the M-ROI method. The intraclass correlation coefficient values for AF increased to 0.378—0.582 for the M-ROI method compared with the 5-ROI method. Comparable results were obtained with Bland—Altman plots.

* Corresponding author. Department of Imaging and Interventional Radiology, Prince of Wales Hospital, The Chinese University of Hong Kong, New Territories, Hong Kong Special Administrative Region.
E-mail address: yixiang_wang@cuhk.edu.hk (Y.X.J. Wang).

http://dx.doi.org/10.1016/j.jot.2016.02.003

Conclusion: The 5-/7-ROI methods agreed with the M-ROI approach for NP selection, while the agreement with AF was moderate to poor, with the 5-ROI method showing slight advantage over the 7-ROI method. Cautions should be taken to interpret the MR relaxometry findings when 5-/7-ROI methods are used to select AF.

Introduction

Intervertebral disc degeneration is the consequence of a variety of genetic, mechanical, traumatic, and nutritional factors, as well as normal ageing [1]. Early signs of disc degeneration are manifested by biochemical changes, including loss of proteoglycans, loss of osmotic pressure, and dehydration [1]. In the later stages of disc degeneration, morphological changes occur, including loss of disc height, disc herniation, annular tears, and radial bulging [2]. Elderly women tend to have more severe disc degeneration than elderly men, and elderly women are more likely to have a narrow lumbar disc space than elderly men [3—5]. Magnetic resonance imaging (MRI) has become the standard noninvasive imaging modality to assess intervertebral discs [2,6—19]. Morphologically, on T2-weighted MR images, disc degeneration is seen as a reduction in the signal of the nucleus pulposus (NP) and inner fibres of the annulus.

The Pfirrmann 5-level grading system is widely used for the evaluation of disc degeneration on MR images [20]. To increase the discriminatory power, the Pfirrmann system has been modified by increasing the number of grades from 5 to 8 [21]. While the 5- and 8-level grading systems provide semiquantitative evaluation of disc degeneration, quantitative MR T2 relaxation time, T1rho relaxation time, and glycosaminoglycan chemical exchange saturation transfer (gag-CEST) measurements of the disc reflect the intrinsic material properties of disc tissues [17,22—30]. These molecular imaging approaches may have the potential to detect subtle differences in tissue composition that may not be apparent in T2-weighted image anatomical assessment and, therefore, would probably be more useful for detecting early disc changes.

T2 relaxation time measurement has been reported to be sensitive to changes in collagen and water content in intervertebral discs, and T2 relaxation time decreases with disc degeneration [17,22—24]. By contrast, T1rho relaxation measurement, which probes the interaction between water molecules and their macromolecular environment, is suggested to have the potential to identify early biochemical changes in intervertebral discs. It was shown that T1rho strongly correlates with proteoglycan content in NP in cadaveric human discs [25]. *In vivo* studies also demonstrated differences in mean T1rho values between NP and annulus fibrosus (AF), and a correlation between T1rho values and degenerative grades was observed [14,26—28]. It has been shown that gag-CEST indicates a correlation between gag-CEST measurement and glycosaminoglycan concentrations. As disc degeneration increases, gag-CEST in NP decreases [29—31].

Recently, MR relaxation time-based techniques and their relationship to disc degeneration [8,12,15,18], dehydration [19], diurnal changes of composition [16], and other functional disc mechanics such as stiffness [11] have been investigated. However, the role of specific biochemical changes in the altered MR signal intensity is still not well understood. An articular cartilage study showed that the loss of proteoglycan results in an increase in T1rho relaxation time [32]. By contrast, T1rho is reported to increase with sulfated glycosaminoglycan content in degenerative discs [17]. The AF functions as a rigid containment for the NP, which is composed of abundant sulfated glycosaminoglycans in a loose network of Type II collagen. It is a hydrated gel containing approximately 25% (dry weight) of collagen and 50% (dry weight) of proteoglycan [33]. Proteoglycans of the nucleus osmotically exert a "swelling pressure", which enables it to support spinal compressive loads. By comparison, AF is made up of coarse Type I collagen fibres, and contains 67% (dry weight) of collagen and a low concentration of proteoglycans [22,33]. During the initial phase of disc degeneration, loss of proteoglycans and Type II collagen in NP is observed [34]. Proteoglycan loss reduces the capacity of NP to bind water and leads to loss of hydration. Later, Type I collagen fibres replace Type II collagen fibres in NP. Tensile properties of the AF tissues are also altered in degenerated discs [35]. On T2-weighted images, T2 map, or T1rho map, both NP and inner AF show nearly the same level of high signal intensity, and the boundary between inner AF and NP is often indistinct [14,30,36—38].

It was suggested that discs can be characterized by T2 mapping and that changes in the integrity of the discs can be assessed before there is a change in the Pfirrmann score [23,32]. However, accurate MR relaxivity mapping at spine discs can be difficult due to the extensive susceptibility effect in the regions. With disc degeneration, the collagen lamellae of the AF increase in thickness and become fibrillated. It is known that AF degeneration is a critical factor in disc stability [2]. In the lumbar spine, the posterior AF is particularly a target for disc abnormalities. For example, annular tears can be identified in MR images by the presence of a high-intensity zone in the posterior AF, which is a marker of a painful posterior annular tear [39]. Recently, Ogon et al [40] reported that the T2 relaxation time of the discs tended to be lower in chronic low back pain patients, and these values were significantly different within the posterior AF. However, chronic low back pain did not show correlations with T2 values in the anterior AF or NP, because of low sensitivity against noxious stimuli in the front part of the disc. This finding further heightens the importance of accurate disc component segmentation, as

targeted tissue regeneration treatment may be possible in the future.

For MR image analysis, a number of methods have been described in literatures to define NP and AF, including the manual region-of-interest (ROI) method based on radiologists' experience, or uniform methods based on equal areas of square or circular ROIs placed horizontally across the disc, with or without a gap between them. For the latter method, the central three ROIs were usually defined as NP, while the anterior or posterior ROIs were defined as the anterior or posterior AF, respectively [6–8,11,13,15–18]. To ensure the accuracy of the T2 and T1rho relaxation times, and CEST technique-based glycosaminoglycan measurement and the subsequent clinical diagnosis as well as early novel treatment [41–43], it is conceptually important to differentiate between NP and AF on these quantitative MR images correctly. Although a consensus has not yet been reached regarding the definition of NP and AF in disc studies, the goals of this work are to evaluate the agreements among different ROI methods and to provide some clarification of ROI definition for further quantitative disc analysis.

Materials and methods

Participants

There were 52 participants in this study: 12 without low back pain (9 males and 3 females; mean age, 32.1 years; age range, 23–42 years) and 40 having low back pain (17 males and 23 females; mean age, 54.1 years; age range, 28–76 years). Based on history, medical records, clinical presentation, and also MRI findings, except disc degeneration, all participants were confirmed to have no active spine lesions such as tumour, infection, autoimmune diseases, etc. This study was approved by the local human research ethics committee, with written informed consents obtained from all participants.

MRI acquisition

All participants underwent imaging in the morning using a 3-T clinical MRI system (Achieva; Philips Healthcare, Best, The Netherlands). A 12-channel receive-only spine coil was used as the signal receiver to cover the lumbar spine, and the built-in body coil was used as the signal transmitter. Volume shimming was employed to minimize B_0 heterogeneity.

For T1rho measurement, a rotary echo spin-lock pulse was implemented in a three-dimensional balanced fast field echo (b-FFE) [35], with a spin-lock frequency of 500 Hz and the spin-lock times (TSLs) of 1 millisecond, 10 milliseconds, 20 milliseconds, 30 milliseconds, 40 milliseconds, and 50 milliseconds. Segmented phase alternating b-FFE readout with centric phase encoding order was used for acquisition. T1rho-weighted images were acquired during the transient status towards the steady state, while maintaining T1rho-weighted magnetization [44]. The rotary echo spin-lock pulse was applied once for every segment length of 80 readouts. A dummy delay time of 6000 milliseconds was inserted after each segment acquisition to fully restore the equilibrium magnetization before the next T1rho preparation. The echo time (TE) and repetition time for b-FFE acquisition were 2.3 milliseconds and 4.6 milliseconds, respectively. The field of view was 200 mm and the pixel size was 1.0 mm × 1.0 mm. Seven sagittal slices were acquired, and the slice thickness was 4 mm. The flip angle was 40° and the number of signal averages was 1. A sensitivity-encoding factor of 2 was applied for parallel imaging to reduce the phase encoding steps. A multiecho turbo spin echo (TSE) pulse sequence was used for T2 mapping. Seven sagittal TSE images were acquired at identical locations as T1rho images. The TSE imaging parameters included the following: field of view = 200 mm; pixel size = 1.0 mm × 1.0 mm; slice thickness = 4 mm; echo train length = 7; TEs = 16 milliseconds, 32 milliseconds, 48 milliseconds, 64 milliseconds, 80 milliseconds, 96 milliseconds, and 112 milliseconds; repetition time = 2300 milliseconds; number of signal averages = 2; and the sensitivity-encoding factor = 2.

Image analysis

The T1rho and T2 maps were computed on a pixel-by-pixel basis using a monoexponential decay model with a homemade Matlab program (Mathworks, Natick, MA, USA):

$$M(TSL) = M0*\exp(-TSL/T1rho) \quad (1)$$

and

$$M(TE) = M0*\exp(-TE/T2) \quad (2)$$

where M0 and M(TSL) denote the equilibrium magnetization and T1rho-prepared magnetization acquired with TSL, respectively. M(TE) denotes the magnetization acquired with TE.

These two monoexponential equations were linearized by logarithm. The T1rho and T2 maps were generated by fitting each pixel's intensity as a function of TSL and TE using a non-negative least-square fitting algorithm, respectively. The T1rho and T2 values were calculated as the inverse of the slope of the corresponding straight-line fit [45].

Five intervertebral discs (L1/L2–L5/S1) per participant were examined, with four discs being excluded because of previous vertebral fusion operation, amounting to a total of 256 discs for analysis. The midsagittal images of the lumbar spine were analysed. The corresponding T2-weighted image was used as the reference for drawing the ROIs. For the manual ROI-based method (M-ROI) [13,14,46], ROIs were manually drawn over the T2-weighted image and copied to the T2 and T1rho maps of the discs by a radiologist with 5 years of experience in reading spine MR images. Three ROIs, including NP, anterior AF, and posterior AF, were drawn (Figure 1A). For the manual ROI placement, the emphasis was on correct sampling of more central parts of targeted issues (i.e., anterior AF, NP, and posterior AF) rather than being very inclusive; this would likely avoid signal contamination by untargeted issues. In addition to radiological experience, the following assumptions were made: (1) a clear separation of NP and inner AF was not possible based on MR images, which would be particularly the case

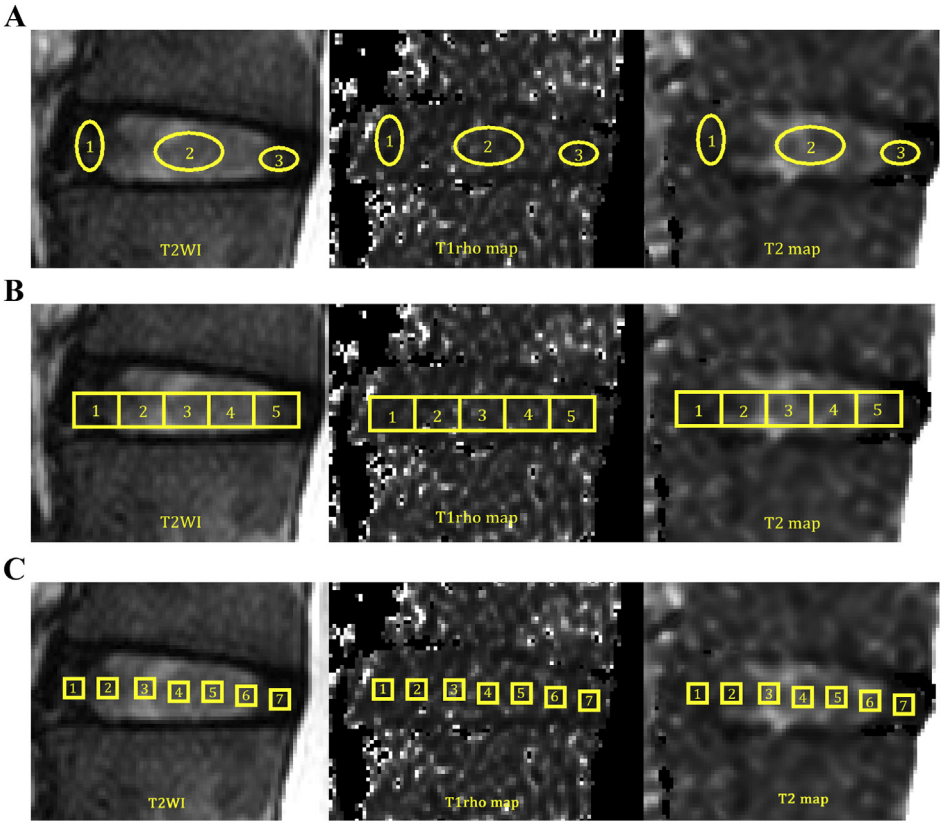

Figure 1 Three ROI drawing methods used in this study: (A) M-ROI, where ROI_1 represents anterior AF, ROI_2 represents NP, and ROI_3 represents posterior AF; (B) 5-ROI; and (C) 7-ROI methods. AF = annulus fibrosus; M-ROI = radiologist-guided manual region of interest; ROI = region of interest; T2WI = T2-weighted image; 5-ROI = five square regions of interest where each measured 20% of the midline disc diameter; 7-ROI = seven square regions of interest placed horizontally from anterior to posterior.

for degenerated discs, and therefore, some space was not included between ROI of NP and ROIs of AF; (2) the endplates, and the anterior and posterior ligaments would all appear as dark signals on T2-weighted images, and separation of these components and AF would not be possible; therefore, sufficient space was allowed for dark signal band near the endplate, near the anterior border close to the abdominal fat of white/grey signal, and near the posterior border close to the bright cerebral spinal fluid signal; and (3) it was considered that the inner AF signal may appear similar to the NP signal. In this study, the manual ROIs were all of oval shape, but they can also have the shape of a polygon, as shown in Figure S1. When an apparent tear was noted in a disc, the abnormal signal areas were excluded from the ROIs. The ROI size for NP ranged from 15 mm^2 to 45 mm^2, while the ROI size for AF (anterior + posterior) ranged from 8 mm^2 to 45 mm^2. For the uniform methods, we evaluated the following methods: (1) 5-ROI method, where each of five equal squares measuring 20% of the midline disc diameter in the sagittal plane [6–8] (Figure 1B) and (2) 7-ROI method, where seven equal squares of 6.5 mm^2 ROI with equal spacing between the ROIs were placed horizontally from anterior to posterior (Figure 1C) [17]. For both the 5-ROI and 7-ROI methods, the average of the central three ROIs was defined as NP, i.e., the second, third, and fourth ROIs for the 5-ROI method, and the third, fourth, and fifth ROIs for the 7-ROI method. Different choices of ROIs were evaluated for defining AF in the 5-ROI method: (1) the first ROI was defined as the anterior AF, and the last ROI was defined as the posterior AF, and (2) average of the first and last ROIs was defined as AF. For the 7-ROI method, the definition of AF includes the following: (1) the first ROI represents the anterior AF and the last ROI represents the posterior AF; (2) average of the first and second ROIs represents the anterior AF, while that of the sixth and seventh ROI represents the posterior AF; and (3) average of the first two and last two ROIs represents AF. The 5-/7-ROI methods were performed using open source image processing software (Image J; National Institutes of Health, Bethesda, MD, USA) [47], while the M-ROI method was performed on a radiological workstation (ViewForum; Philips Medical Systems Nederland B.V., a Philips Healthcare Company, Best, The Netherlands).

The agreement between the M-ROI, 5-ROI, and 7-ROI methods was assessed, using intraclass correlation coefficient (ICC) on absolute agreement as well as Bland–Altman plots. According to Fleiss, ICC values of > 0.75 represent a good agreement, and values between 0.4 and 0.75 represent a fair-to-moderate agreement [48].

Results

The ICC and Bland–Altman plot results comparing the three methods are shown in Tables 1–4 and Figures S2–21. Inner AF and NP could not be differentiated on T1/T2-weighted

Table 1 ICC values for comparing M-ROI and 7-ROI methods to define NP and AF.

	Central 3 ROIs[a]	1st & 2nd ROIs[b]	1st ROI[c]	6th & 7th ROIs[d]	7th ROI[e]	1st, 2nd, 6th, & 7th ROIs[f]
T2	0.799	0.256	0.193	0.167	0.351	0.201
T1rho	0.765	0.392	0.397	0.486	0.466	0.488

AF = annulus fibrosus; ICC = intraclass correlation coefficient; M-ROI = radiologist-guided manual region of interest; NP = nucleus pulposus; ROI = region of interest; 7-ROI = seven square regions of interest placed horizontally from anterior to posterior.
[a] The mean of central three ROIs was taken as NP.
[b] The mean of the first and second ROIs was taken as anterior AF.
[c] The mean of the first ROI was taken as anterior AF.
[d] The mean of the sixth and seventh ROIs was taken as posterior AF.
[e] The mean of the seventh ROI was taken as posterior AF.
[f] The mean of the first, second, sixth, and seventh ROIs was taken as AF.

MRI, T2 maps, or T1rho maps. The trend showed that when the average of the two measurements was big, the difference between the two measurements was also bigger. The ICC values were all > 0.75 when comparing the 5-/7-ROI methods with the M-ROI methods for NP. However, the agreement for assessing AF was only moderate or poor (Tables 1 and 2). Compared with the 7-ROI method, the results were slightly in favour of the 5-ROI method (Tables 1 and 2). Selecting the first and the seventh ROIs as the anterior and posterior AF, respectively, did not improve the agreement between the 7-ROI and M-ROI methods, as compared with using the average of the two ROIs to represent anterior/posterior AF. Comparable results were obtained with Bland–Altman plots (Tables 3 and 4, and Figures S2–21).

Discussion

It is known that the common 5-ROI method cannot exclude annular tears, and there is high possibility that a portion of inner AF is included as NP. While inner AF is distinct from NP histologically, so far T2-weighted anatomical images, T2 and T1rho relaxation maps, and gag-CEST map have failed to separate inner AF distinctly from NP [30]. Although the 5- or 7-ROI methods may help in automatic or semiautomatic image analysis, potentially reducing radiologists' workload [17,49], there is a probability that in the 5-ROI method, the first and fifth ROIs are contaminated with signals from anterior and posterior longitudinal ligaments, and endplates. The border between AF and NP is unlikely to be vertical as delineated in the 5-ROI methods; the shape of NP and AF changes due to ageing and degeneration, but the 5-/7-ROI methods could not account for this. It has also been noted that in the lumbar spine, AF tends to be thicker ventrally than dorsally [50]. The M-ROI method, as described in our methodology, is more likely to select the "pure" NP and AF components, allowing more accurate studies of degeneration-related mechanisms of these components. With the 7-ROI method, we initially hypothesized that while the second and sixth ROIs might include some of the NP components, the first and seventh ROIs would represent AF better. However, our results did not show that the first and seventh ROIs had good agreement with M-ROI measurements for AF either. Owing to the lower water and GAG contents and a higher collagen content of the AF, the T2 time and T1rho time are on average lower; consequently, the random variation in these regions of the discs will generate more "noise" relative to the mean value. As T2 mapping and T1rho mapping are likely to have lower signal-to-noise ratios, the 7-ROI method with a smaller number of pixels is likely to have less accuracy; in addition, as shown in Figure 1C, some areas of AF and NP are not fully utilized for measurement. The first and seventh ROIs would suffer from the same signal contaminations as the first and fifth ROIs in the 5-ROI method. In addition, the principle described above would also apply to disc MRI in the axial plane. Further researches, using the histogram method excluding extremely low signals from endplates and using multiparametric techniques such as ultrashort echo time, may help in disc tissue segmentation. It is also possible that the development of future MR-based molecular imaging techniques will allow better differentiation of disc tissue components.

This study showed the potential imprecision of the 5-/7-ROI methods and a moderate-to-poor agreement with the M-ROI method for defining AF. One limitation of the present study is the lack of a gold standard. Understandably, no histological samples could be obtained. Nevertheless, in this study, we assumed that the manual method guided by an experienced radiologist would allow correct selection of the cores of the NP and AF. Ideally, the ROI methods should include all components of the discs while maintaining a separation between NP and AF. However, it is not possible with current MRI technology to clearly separate the whole NP and whole AF; therefore, anatomical knowledge-based manual segmentation remains the most reliable method.

Table 2 ICC values for comparing M-ROI and 5-ROI methods to define NP and AF.

	Central three ROIs[a]	1st ROI[b]	5th ROI[c]	1st & 5th ROIs[d]
T2	0.911	0.476	0.398	0.460
T1rho	0.806	0.378	0.582	0.508

AF = annulus fibrosus; ICC = intraclass correlation coefficient; M-ROI = radiologist-guided manual region of interest; NP = nucleus pulposus; ROI = region of interest; 5-ROI = five square regions of interest where each measured 20% of the midline disc diameter.
[a] The mean of central three ROIs was taken as NP.
[b] The mean of the first ROI was taken as anterior AF.
[c] The mean of the fifth ROI was taken as posterior AF.
[d] The mean of the first and fifth ROIs was taken as AF.

Table 3 Bland–Altman plot results comparing T2 and T1rho values measured by M-ROI and 5-ROI methods.

	Mean difference (T2/T1rho)	95% limits of agreement (upper limit) (T2/T1rho)	95% limits of agreement (lower limit) (T2/T1rho)
NP versus mean of central 3 ROIs	3.526/0.874	31.707/35.969	−24.654/−34.221
Anterior AF versus 1st ROI	−3.828/−4.313	23.260/22.630	−30.917/−31.256
Posterior AF versus 5th ROI	−3.828/−10.949	14.377/18.988	−22.034/−40.886
AF versus mean of 1st & 5th ROIs	−3.828/−7.631	14.326/14.303	−21.982/−29.565

AF = annulus fibrosus; M-ROI = radiologist-guided manual region of interest; NP = nucleus pulposus; ROI = region of interest; 5-ROI = five square regions of interest where each measured 20% of the midline disc diameter.

Table 4 Bland–Altman plot results comparing T2 and T1rho values measured by M-ROI and 7-ROI methods.

	Mean difference (T2/T1rho)	95% limits of agreement (upper limit) (T2/T1rho)	95% limits of agreement (lower limit) (T2/T1rho)
NP versus mean of central 3 ROIs	−0.521/0.136	39.146/34.561	−40.188/−34.289
Anterior AF versus 1st ROI	2.359/−2.146	30.511/26.558	−25.792/−30.849
Anterior AF versus mean of 1st & 2nd ROIs	−6.701/−6.875	20.81/21.992	−34.213/−35.743
Posterior AF versus 7th ROI	−3.918/−1.855	21.116/18.696	−28.953/−22.406
Posterior AF versus mean of 6th and 7th ROIs	−18.488/−7.398	15.516/13.049	−52.493/−27.845
AF versus mean of 1st, 2nd, 6th, & 7th ROIs	−12.595/−7.120	11.403/10.418	−36.593/−24.657

AF = annulus fibrosus; M-ROI = radiologist-guided manual region of interest; NP = nucleus pulposus; ROI = region of interest; 7-ROI = seven square regions of interest placed horizontally from anterior to posterior.

In conclusion, this study shows that the commonly used 5-/7-ROI methods agreed with the radiologist-guided manual ROI approach for NP selection, but this could be due to the fact that there is no substantial difference between T2 and T1rho values of inner AF and NP. The importance of separation of inner AF and NP also remains to be further defined [51]. The agreement between the three methods regarding AF was only poor to moderate. The 7-ROI method did not improve the selection for AF compared with the 5-ROI method. Overall, based on the results of this study, as well as the histological difference between inner AF and NP, we do not support the use of the 5-/7-ROI methods for segmentation of AF and NP. To better understand the differences between T1rho and T2 relaxation time reduction during the course of NP and AF degeneration, and to translate these relaxation times into reliable and specific biomarkers for early disc degeneration, a more precise, reproducible, and inclusive method for AF selection remains to be further developed. For the time being, we advocate manual ROI segmentation of AF and NP by experienced radiologists.

Conflicts of interest

All authors declare that they have no conflicts of interest.

Funding/support

This study was partially supported by a grant from the Research Grants Council of the Hong Kong SAR (No. SEG-CUHK02) and a research grant from the University of Macau, Macau SAR [MYRG185(Y3-L3)-FST11-MSP].

Acknowledgements

We thank Drs Min Deng and Feng Zhao for their assistance with image processing.

Appendix A. Supplementary data

Supplementary data related to this article can be found at http://dx.doi.org/10.1016/j.jot.2016.02.003.

References

[1] Adams MA, Roughley PJ. What is intervertebral disc degeneration, and what causes it? Spine 2006;31:2151–61.
[2] Modic MT, Ross JS. Lumbar degenerative disk disease. Radiology 2007;245:43–61.
[3] Wáng YX, Griffith JF, Ma HT, Kwok AWL, Leung JCS, Yeung DW, et al. Relationship between gender, bone mineral density, and disc degeneration in the lumbar spine: a study in elderly subjects using an eight-level MRI-based disc degeneration grading system. Osteoporos Int 2011;22:91–6.
[4] Wáng YX, Griffith JF. Effect of menopause on lumbar disk degeneration: potential etiology. Radiology 2010;257:318–20.
[5] Wáng YX, Griffith JF, Zeng XJ, Deng M, Kwok AW, Leung JC, et al. Prevalence and sex difference of lumbar disc space narrowing in elderly Chinese men and women: osteoporotic fractures in men (Hong Kong) and osteoporotic fractures in women (Hong Kong) studies. Arthritis Rheum 2013;65:1004–10.
[6] Stelzeneder D, Welsch GH, Kovács BK, Goed S, Paternostro-Sluga T, Vlychou M, et al. Quantitative T2 evaluation at 3.0T compared to morphological grading of the lumbar intervertebral disc: a standardized evaluation approach in patients with low back pain. Eur J Radiol 2012;81:324–30.

[7] Trattnig S, Stelzeneder D, Goed S, Reissegger M, Mamisch TC, Paternostro-Sluga T, et al. Lumbar intervertebral disc abnormalities: comparison of quantitative T2 mapping with conventional MR at 3.0 T. Eur Radiol 2010;20:2715—22.
[8] Takashima H, Takebayashi T, Yoshimoto M, Terashima Y, Tsuda H, Ida K, et al. Correlation between T2 relaxation time and intervertebral disk degeneration. Skelet Radiol 2012;41:163—7.
[9] Kwok AWL, Wáng YX, Griffith JF, Deng M, Leung JC, Ahuja AT, et al. Morphological changes of lumbar vertebral bodies and intervertebral discs associated with decrease in bone mineral density of the spine: a cross-sectional study in elderly subjects. Spine 2012;37:1415—21.
[10] Wáng YX, Kwok AW, Griffith JF, Leung JC, Ma HT, Ahuja AT, et al. Relationship between hip bone mineral density and lumbar disc degeneration: a study in elderly subjects using an eight-level MRI-based disc degeneration grading system. J Magn Reson Imaging 2011;33:916—20.
[11] Ellingson AM, Mehta H, Polly DW, Ellermann J, Nuckley DJ. Disc degeneration assessed by quantitative T2* (T2 star) correlated with functional lumbar mechanics. Spine 2013;38:1533—40.
[12] Wáng YX, Griffith JF, Leung JCS, Yuan J. Age related reduction of T1rho and T2 magnetic resonance relaxation times of lumbar intervertebral disc. Quant Imaging Med Surg 2014;4:4259—64.
[13] Marinelli NL, Haughton VM, Muñoz A, Anderson PA. T2 relaxation times of intervertebral disc tissue correlated with water content and proteoglycan content. Spine 2009;34:520—4.
[14] Wáng YX, Zhao F, Griffith J, Mok GS, Leung JC, Ahuja AT, et al. T1rho and T2 relaxation times for lumbar disc degeneration: an *in vivo* comparative study at 3.0-Tesla MRI. Eur Radiol 2013;23:228—34.
[15] Welsch G, Trattnig S, Paternostro-Sluga T, Bohndorf K, Goed S, Stelzeneder D, et al. Parametric T2 and T2* mapping techniques to visualize intervertebral disc degeneration in patients with low back pain: initial results on the clinical use of 3.0 Tesla MRI. Skelet Radiol 2011;40:543—51.
[16] Ludescher B, Effelsberg J, Martirosian P, Steidle G, Markert B, Claussen C, et al. T2- and diffusion-maps reveal diurnal changes of intervertebral disc composition: an *in vivo* MRI study at 1.5 Tesla. J Magn Reson Imaging 2008;28:252—7.
[17] Chiu EJ, Newitt DC, Segal MR, Hu SS, Lotz JC, Majumdar S. Magnetic resonance imaging measurement of relaxation and water diffusion in the human lumbar intervertebral disc under compression *in vitro*. Spine 2001;26:437—44.
[18] Antoniou J, Epure LM, Michalek AJ, Grant MP, Iatridis JC, Mwale F. Analysis of quantitative magnetic resonance imaging and biomechanical parameters on human discs with different grades of degeneration. J Magn Reson Imaging 2013;38:1402—14.
[19] Niinimäki J, Ruohonen J, Silfverhuth M, Lappalainen A, Kääpä E, Tervonen O. Quantitative magnetic resonance imaging of experimentally injured porcine intervertebral disc. Acta Radiol 2007;48:643—9.
[20] Pfirrmann CW, Metzdorf A, Zanetti M, Hodler J, Boos N. Magnetic resonance classification of lumbar intervertebral disc degeneration. Spine 2001;26:1873—8.
[21] Griffith JF, Wáng YX, Antonio GE, Choi KC, Yu A, Ahuja AT, et al. Modified Pfirrmann grading system for lumbar intervertebral disc degeneration. Spine 2007;32:708—12.
[22] Weidenbaum M, Foster RJ, Best BA, Saed-Nejad F, Nickoloff E, Newhouse J, et al. Correlating magnetic resonance imaging with the biochemical content of the normal human intervertebral disc. J Orthop Res 1992;10:552—61.
[23] Kerttula L, Kurunlahti M, Jauhiainen J, Koivula A, Oikarinen J, Tervonen O. Apparent diffusion coefficients and T2 relaxation time measurements to evaluate disc degeneration. Acta Radiol 2001;42:585—91.
[24] Perry J, Haughton V, Anderson PA, Wu Y, Fine J, Mistretta C. The value of T2 relaxation times to characterize lumbar intervertebral disks: preliminary results. Am J Neuroradiol 2006;27:337—42.
[25] Johannessen W, Auerbach JD, Wheaton AJ, Kurji A, Borthakur A, Reddy R, et al. Assessment of human disc degeneration and proteoglycan content using T1ρ-weighted magnetic resonance imaging. Spine 2006;31:1253—7.
[26] Blumenkrantz G, Li X, Han ET, Newitt DC, Crane JC, Link TM, et al. A feasibility study of *in vivo* T1ρ imaging of the intervertebral disc. Magn Reson Imaging 2006;24:1001—7.
[27] Auerbach J, Johannessen W, Borthakur A, Wheaton AJ, Dolinskas CA, Balderston RA, et al. *In vivo* quantification of human lumbar disc degeneration using T1ρ-weighted magnetic resonance imaging. Eur Spine J 2006;15:338—44.
[28] Blumenkrantz G, Zuo J, Li X, Kornak J, Link TM, Majumdar S. *In vivo* 3.0-tesla magnetic resonance T1ρ and T2 relaxation mapping in subjects with intervertebral disc degeneration and clinical symptoms. Magn Reson Med 2010;63:1193—200.
[29] Müller-Lutz A, Schleich C, Pentang G, Schmitt B, Lanzman RS, Matuschke F, et al. Age-dependency of glycosaminoglycan content in lumbar discs: a 3T gagcEST study. J Magn Reson Imaging 2015;42:1517—23.
[30] Deng M, Yuan J, Chen WT, Chan Q, Griffith JF, Wáng YX. Evaluation of glycosaminoglycan in the lumbar disc using chemical exchange saturation transfer MR at 3.0 Tesla: reproducibility and correlation with disc degeneration. Biomed Environ Sci 2016;29:47—55.
[31] Liu Q, Jin N, Fan Z, Natsuaki Y, Tawackoli W, Pelled G, et al. Reliable chemical exchange saturation transfer imaging of human lumbar intervertebral discs using reduced-field-of-view turbo spin echo at 3.0 T. NMR Biomed 2013;26:1672—9.
[32] Akella SVS, Regatte R, Gougoutas AJ, Borthakur A, Shapiro EM, Kneeland JB, et al. Proteoglycan-induced changes in T1ρ-relaxation of articular cartilage at 4T. Magn Reson Med 2001;46:419—23.
[33] Cassinelli EH, Hall RA, Kang JD. Biochemistry of intervertebral disc degeneration and the potential for gene therapy applications. Spine J 2001;1:205—14.
[34] Antoniou J, Steffen T, Nelson F, Winterbottom N, Hollander AP, Poole RA, et al. The human lumbar intervertebral disc: evidence for changes in the biosynthesis and denaturation of the extracellular matrix with growth, maturation, ageing, and degeneration. J Clin Invest 1996;98:996—1003.
[35] Charagundla SR, Borthakur A, Leigh JS, Reddy R. Artifacts in T1ρ-weighted imaging: correction with a self-compensating spin-locking pulse. J Magn Reson 2003;162:113—21.
[36] Inoue N, Espinoza Orías AA. Biomechanics of intervertebral disk degeneration. Orthop Clin North Am 2011;42:487—99.
[37] Haughton VM. Chapter 6: Age-related changes in the spine. In: Naidich TP, Castillo M, Cha S, Raybaud C, Smirniotopoulos JG, Kollias S, editors. Imaging of the spine. 1st ed. Philadelphia: Saunders Elsevier; 2011. p. 147—60.
[38] Wang YX. Inner annulus fibrosus in non-degenerated intervertebral disc shows bright signal on T2 weighted MR image. Quant Imaging Med Surg 2014;4:504.
[39] Peng B, Hou S, Wu W, Zhang C, Yang Y. The pathogenesis and clinical significance of a high-intensity zone (HIZ) of lumbar intervertebral disc on MR imaging in the patient with discogenic low back pain. Eur Spine J 2006;15:583—7.
[40] Ogon I, Takebayashi T, Takashima H, Tanimoto K, Ida K, Yoshimoto M, et al. Analysis of chronic low back pain with magnetic resonance imaging T2 mapping of lumbar intervertebral disc. J Orthop Sci 2015;20:295—301.
[41] Phillips FM, An H, Kang JD, Boden SD, Weinstein J. Biologic treatment for intervertebral disc degeneration: summary statement. Spine 2003;28:S99.

[42] Vadalà G, Sowa GA, Kang JD. Gene therapy for disc degeneration. Expert Opin Biol Ther 2007;7:185—96.
[43] Carl A, Ledet E, Yuan H, Sharan A. New developments in nucleus pulposus replacement technology. Spine J 2004;4:325S—9S.
[44] Li X, Han ET, Busse RF, Majumdar S. *In vivo* T1ρ mapping in cartilage using 3D magnetization-prepared angle-modulated partitioned k-space spoiled gradient echo snapshots (3D MAPSS). Magn Reson Med 2008;59:298—307.
[45] Wáng YX, Yuan J, Chu ES, Go MY, Huang H, Ahuja AT, et al. T1ρ MR imaging is sensitive to evaluate liver fibrosis: an experimental study in a rat biliary duct ligation model. Radiology 2011;259:712—9.
[46] Wáng YX, Zhao F, Yuan J, Mok GSP, Ahuja AT, Griffith JF. Accelerated T1rho relaxation quantification in intervertebral disc using limited spin-lock times. Quant Imaging Med Surg 2013;3:54—8.
[47] Schneider CA, Rasband WS, Eliceiri KW. NIH image to ImageJ: 25 years of image analysis. Nat Meth 2012;9:671—5.
[48] Fleiss JL. The design and analysis of clinical experiments. New York: John Wiley & Sons; 1986.
[49] Michopoulou SK, Costaridou L, Panagiotopoulos E, Speller R, Panayiotakis G, Todd-pokropek A. Atlas-based segmentation of degenerated lumbar intervertebral discs from MR images of the spine. IEEE Trans Biomed Eng 2009;56:2225—31.
[50] Carrino JA, Morrison WB. Imaging of lumbar degenerative disc disease. Semin Spine Surg 2003;15:361—83.
[51] Wáng YX, Zhang Q, Li X, Chen W, Ahuja A, Yuan J. T1ρ magnetic resonance: basic physics principles and applications in knee and intervertebral disc imaging. Quant Imaging Med Surg 2015;5:858—85.